ISSN 1027-5495. Functional Materials, 30, No.1 (2023), p. 65-73.
doi:https://doi.org/10.15407/fm30.01.65

Comparing of the characteristics of thermal spray coating technologies: air-fuel detonation aluminum spraying onto steel with other technologies

***K.V.Korytchenko*[1], *V.Yu.Kucherskyi*[1], *R.Y.Krasnoshapka*[1], *D.P.Dubinin*[2], *S.M.Shevchenko*[2], *R.I.Kovalenko*[2]**

[1]National Technical University "Kharkiv Polytechnic Institute",
2 Kyrpychova Str., 61002 Kharkiv, Ukraine
[2]National University of Civil Defence of Ukraine, 94 Chernyshevska Str.,
61023 Kharkiv, Ukraine

Received November 26, 2022

In this paper, on the basis of data obtained for the deposition of aluminum on steel, the characteristics of the air-fuel detonation technology used for thermal spraying are compared with similar technologies. The measurement data show that the pressure of the detonation products in the airfuel detonation technology reaches 1.68 MPa. The temperature of detonation products varies in the range of 1845 to 2200 K. The comparison was made on coating parameters such as porosity, adhesion, surface roughness and cost. It has been established that the developed air-fuel detonation technology has certain advantages related to porosity and productivity. However, this technological process requires certain improvement to increase adhesion and decrease roughness.
Keywords: gas-detonation spraying, air-fuel technology, spraying aluminum onto steel.

Порівняння показників паливо-повітряної технології газотедонаційного напилювання з показниками аналогічних технологій за результатами нанесення алюмінію на сталь. *К.В.Коритченко, В.Ю.Кучерський, Р.Ю.Красношапка, Д.П.Дубінін, С.М.Шевченко, Р.І.Коваленко*

В роботі проведено порівняння показників паливо-повітряної технології газотедонаційного напилювання з показниками аналогічних технологій за результатами нанесення алюмінію на сталь. Встановлено, що тиск продуктів детонації досягає 1,68 МПа. Визначено, що температура продуктів детонації перебуває в межах 1845 і 2200 К. Порівняння показників здійснено за параметрами пористості покриття, адгезії, шорсткості поверхні та вартості. Показано переваги розробленої технології щодо пористості та продуктивності. Разом з тим потребує удосконалення технологічний процес для підвищення адгезії та зниження шорсткості.

1. Introduction

The thermal spraying is widely used for the improvement of the properties of different products by applying the coatings of one material onto another material [1–5]. Continuous improvement of this spraying technology is aimed at improving adhesion [6], reducing the porosity of the coating [7], minimizing changes in the quality of the coating material [8, 9], increasing the efficiency of spraying and reducing its cost, including manufacturability, etc. The development of thermal spray technologies is aimed at universalization by increasing the number of advantages in spray characteristics [10, 11].

Recently, high-speed oxy-fuel spraying has the greatest advantages in terms of the ratio of such characteristics as quality, productivity and manufacturability. At the same time, the gas-detonation spraying is considered to be more profitable in terms of quality; and the plasma spraying and arc spraying have the lowest cost [12]. The recent development of the technique of the gas detonation initiation has made it possible to improve the technology of the gas-detonation spraying by replacing the fuel-oxygen mixture with an air-fuel mixture. Such an approach creates preconditions for an increase in the efficiency and a decrease in the cost of the gas-detonation technology. However, it is still necessary to consider the issue of maintaining the quality of such a detonation coating by reducing the pressure and temperature of the detonation products in this case. The purpose of this research was to compare the characteristics of the air-fuel detonation technology used for the thermal spraying with those of other spraying technologies for aluminum deposited onto steel.

The article [13] discusses the study of aluminum-coated steel. It has been found that such a coating provides protection to steel subject to water corrosion, such as marine structures and elements that can be damaged due to immersion in sea water, tides and splashes. It should be noted that the aluminum coating of 200μm thick extends the service life up to 30 years of a steel product exposed to aggressive media. The comparison was done using data obtained by sputtering aluminum wire containing 99.5 % aluminum that resulted in the formation of a coating layer of 250 to 300 μm thick on the C–Mn steel substrate ((BS EN 10025:1993:S355J2G4). The following commercial spraying technologies were used [11]: a) installation of wire flame spraying MK73, using propane as a fuel [14]; b) 528 arc spray system with compressed air as carrier gas [15], c) upgraded arc spray system using inert gas (nitrogen) as carrier gas, d) HV_w2000 high-speed wire flame sprayer manufactured by HVT LLC, USA, operating on high pressure propane and air-oxygen mixture. Paper [16] studies the quality of steel coated with an aluminum layer of 200 to 300 μm thick deposited using twin wire arc spraying, in which a DC electric arc between aluminum electrodes leads to electric erosion of electrodes and melted aluminum particles are accelerated by the compressed air and directed to the steel substrate. Prior to thermal spraying, the substrate was prepared to SA 2.5 (ISO8501-1) purity standard by sandblasting with angular aluminum oxide particles (type NK36, 0.250–0.297 mm) under an air pressure of 0.69 MPa. Commercially pure aluminum (alloy 1050, 99.5 mass % Al) in the form of wire with a diameter of 2.3 mm was used for spraying. Carbon steel S355 N, EN 10,025-3:2004 was used as the substrate. The roughness of thermal sprayed aluminum (TSA) coatings was measured using 3D profilometry. The porosity of the coating was determined by image analysis using a threshold color instrument for cross-sectional SEM images. It was established that aluminum coatings applied by this method are able to provide corrosion protection for marine steel structures throughout the period of 20 to 30 years.

In [17], studies of aluminum coatings applied to steel by thermal spraying to reduce the corrosive effect on offshore structures are considered. The substrates were made of low-carbon S355 steel with a purity standard of SA 2.5. Defects imitating metal erosion and mechanical damage were created on steel. Steel was coated with commercially pure aluminum (alloy 1050, 99.5 % aluminum) by arc spraying using an ARC528E gun manufactured by the Metallisation Ltd [18]. The coating thickness varied in the range of 200 to 300 μm. Experiments show that the anticorrosion protection of steel provides the corrosion rate less than 20 μm/year.

In [19], the data of numerical studies of the corrosion resistance of aluminum coatings deposited on a steel substrate by thermal spraying in the case of damage to the surface are presented. The coating thickness varied in the range of 200 to 350 μm. The study was carried out using COMSOL Multiphysics 5.6@ software for 5 %, 50 %, and 90 % damage to coatings. It was established that the service life of the structure exposed to aggressive sea water can exceed 86 years with a small percentage of damage.

In [20], the thermal and cold modes of aluminum spraying are considered, which are used to reduce the corrosive effect on steel structures exposed to sea water. The coating quality was evaluated taking into consideration such parameters as the coating composition, coating density, consequences of damage to the coated surface, the effect of temperature, oxygen and the chemical composition on the coated surface. It was found that an optimal thickness of the aluminum coating is in the range of 150 to 375 μm.

In [21] the comparison of different thermal spray processes is discussed. It was shown that arc spraying has certain advantages in comparison to flame spraying as for the cost and efficiency. It was established that arc spraying provides lower porosity, however the flame spray process is characterized by a lower percentage of oxides.

Hence, we can state that thermal coatings are widely used for the protection of equipment operating in aggressive environments. Particular attention is paid to the aluminum coating, which has found wide application. Different types of spray processes compete to show better qualitative and quantitative indices. This indicates the need to improve technologies, taking into account the totality of the relevant characteristics. Actually, our research was aimed at improving the detonation process, taking into account a number of very important parameters.

2. Experimental

Air-fuel detonation spraying mode and equipment

Detonation spraying was performed using a detonation gun operating on a compressed airpropane mixture; the principle of the gun operation was described in [22–29]. The compressor had a volume of 815 cm^3 and the revolution frequency of 2825 min^{-1}. A commercial propane-butane mixture prepared according to DSTU 4047-2001 was used as a fuel. The detonation tube has a length of 1.2 m and an inner diameter of 20 mm.

The study was carried out taking into account the difference in the conditions for the acceleration of the sprayed gunpowder in the detonation gun used and in the classic propane-oxygen detonation guns. The powder acceleration is defined by the pressure pulse acting on powder particles. Therefore, the pressure change over time was measured at the point of powder supply to the detonation tube. The pressure was measured with a PCB 113B22 pressure sensor and recorded with a RIGOL DS1000E oscilloscope. Fig. 1 gives the pressure measurement data.

The above pressure oscillogram shows three surges of pressure within 50 ms, where the first surge and the third surge (*1*) correspond to the detonation combustion and the second surge (*2*) corresponds to an increase in the pressure during the detonation tube scavenging (Fig. 1). The spark ignition of fuel results in electromagnetic noise signals (*3*). The measurement data show that the maximum pressure during

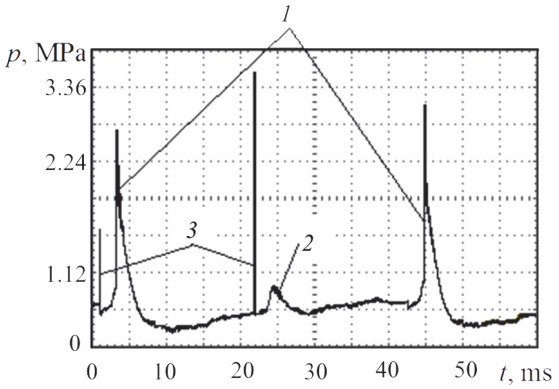

Fig. 1. A change in the relative pressure with time at the point of powder supply to the detonation tube for spraying: *1* — detonation combustion cycles; *2* — scavenging cycle; *3* — electromagnetic noise caused by the spark ignition.

the scavenging attains approximately 340 kPa (cycle 2). Detonation combustion cycles (*1*) are characterized by an abrupt increase in the pressure. However, the compression of the propane-butane gas mixture is observed before the detonation. In addition, the detonation occurs actually at the compression peak. The amplitude value of the pressure in the detonation wave is changed from one cycle to another; however, the mean value is 2.8 MPa. For comparison, the measurement data given in [30] show that the amplitude value of the pressure in the detonation wave, in the case of the stoichiometric oxygen-propane gas mixture, is equal to 2.84 MPa. The data given in [31] show that the pressure of detonation products in the stoichiometric propane-butane gas mixture equals to 1.86 MPa. From this we can conclude that the detonation wave pressure is actually equal to that recorded for the guns using an oxygen-propane gas mixture. Note that the maximum pressure of detonation products in the developed gun is at least 1.7 times higher than the values achieved in guns operating on an uncompressed air-propane mixture [32, 33].

It is known that the combustion temperature of an air-propane mixture is much lower than that of an oxygen-propane mixture. Let us estimate the temperature reached in the developed gun from the pressure measurement data. Let us assume that the adiabatic compression of the mixture occurs before the detonation initiation. In this case, an increase in the mixture density is in a direct proportion to the compression ratio. The compression ratio is derived from the expression

$$\varepsilon = \left(\frac{p_1}{p_0}\right)^{\frac{1}{\gamma}}, \quad (1)$$

where p_0 is the initial mixture pressure; p_1 is the compressed mixture pressure, γ is the adiabatic index.

Taking into consideration an insignificant portion of propane in the mixture, we assume that $\gamma = 1.4$. We have $p_0 = 101.3$ kPa and $p_1 = 340$ kPa according to the measurement data. The initial density of the stoichiometric air-propane mixture is equal to 1.31 kg/m^3. The density of the compressed mixture is increased to $\rho = 3.1$ kg/m^3.

The temperature of detonation products is derived from the expression

$$T = \frac{Mp_2}{\rho R}, \quad (2)$$

where M is a molar mass of detonation products; p_2 is the pressure of detonation products; R is the gas constant.

For the detonation products of a stoichiometric air-propane mixture we get $M = 8.3$ kg/kmole. According to the measurement data, $p_2 = 1.68$ MPa. Based on these data, we obtain the temperature $T = 1845$ K from the equation (2). In this case, for the detonation wave where the pressure reaches 2.8 MPa, the gas temperature is equal to 3076 K according to the expression (2). It should be noted that the obtained temperature data are approximate, since the detonation wave is characterized by a nonuniform distribution of gas density along the coordinate in the direction of wave propagation. In addition, the gas density at the detonation wave front is higher than the density of atmospheric gas; while the density of detonation products behind the detonation wave front is lower. Hence, the actual temperature of detonation products exceeds the calculated temperature value, and the gas temperature in the detonation wave is lower than the calculated value. The relationship of the gas density ?f at the wave front and the initial gas density ρ_f is derived from the expression [34]

$$\frac{\rho_f}{\rho} = \frac{k+1}{k}, \quad (3)$$

where k is the polytropic index.

For the detonation products of the air-propane mixture we assume $k = 1.36$. Hence, we observe an increase in the density by a factor of 1.73. As a result, the gas temperature at the wave front is equal to 1778 K. At the same time, the density of detonation products is lower than the density ρ of atmospheric gas and is equal to 0.78ρ in this case [32]. As a result, we have the temperature of detonation products equal to 2365 K. Based on the obtained data and taking into consideration the specific features of detonation combustion we can assume that the temperature of detonation products in the developed detonation gun is approximately equal to the adiabatic temperature of the flame of the air-propane mixture, which is approximately 2250 K [35].

To ensure high efficiency in the use of the sprayed powder, it is necessary to ensure its timely delivery. Therefore, the time delay between the actuation of the signal applied to the pneumatic valve and the time of gas exit from the powder supply tube was measured.

The response time of the signal applied to the electric pneumovalve was recorded by the first channel of the RIGOL DS1000E oscilloscope with the sweep triggered by the input signal. The dynamic pressure was created during the gas exit. Therefore, the start of the gas exit was measured by a PCB113B22 piezo pressure sensor, the signal of which was fed to the second channel of the oscilloscope. The distance between the piezo pressure sensor and the powder supply tube was 5 mm. Fig. 2 shows the measurement data of the signals of the electric pneumovalve and the piezoelectric sensor.

The measurement data show that the time delay between the actuation of voltage supplied to the pneumatic valve and the start of the gas exit from the powder supply tube is approximately 4...4.2 ms. In this case, the time of the voltage supply of the valve is 6 ms. The pressure pulse time is 6 ms.

The conducted studies and the method of adjusting the detonation gun show that the following modes of the spraying process were provided (see Table 1).

The PAP-1 powder was used for spraying. Table 2 gives basic powder parameters.

Before the spraying process, the sprayed material (the PAP-1 powder) was studied using the microscope to define the shape of particles to be sprayed. Fig. 3 shows the powder particles visualized through the microscope.

The obtained data show that the PAP-1 powder particles have an irregular arbitrary shape. The average linear size of the powder particles is 30±15 μm. The object of spray-

Table 1. Technological conditions for the detonation powder spraying

Parameter	Data
Maximum pressure of detonation products, MPa	1.68
Temperature of detonation products, K	1845–2200
Powder injection time, ms	6
Time delay between the powder supply interruption time and the time of detonation wave coming to the powder injection point, ms	1
Distance from the point of powder injection to the open tube end, mm	300
Distance from the tube end to the covering object, mm	200
Cyclic powder feed, g	0.5
Cycle frequency, Hz	23...24

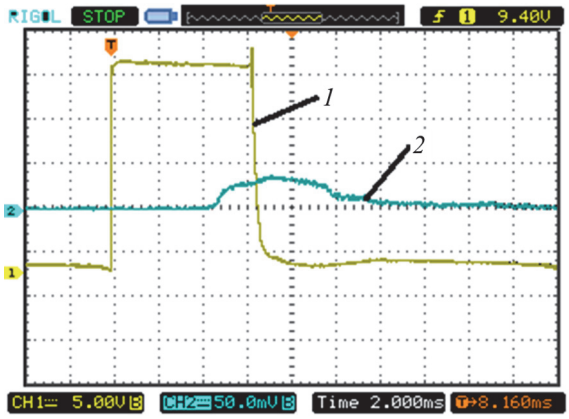

Fig. 2. Delay measurement data: *1* — electric pneumovalve signal; *2* — piezo sensor signal. Time scale is 2 ms/div.

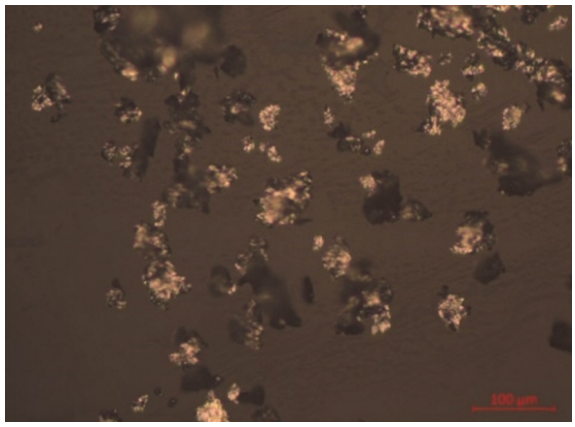

Fig. 3. Image of the PAP-1 powder particles on the glass slide.

ing was the plate made of the carbon structural steel of standard quality.

It should be noted that the PAP-1 powder has a developed surface; this leads to an intense oxidation during gas-thermal spraying. But the proposed spraying technology has a pulsed thermal effect, a lower gas temperature and a lower oxygen concentration. This helps reduce powder burnout. Given the low cost of PAP-1, this powder was used in the above studies.

Porosity investigation methods

The coating porosity was studied using the immersion method [37]. The aluminum-coated sample was immersed into the solution of potassium ferricyanide — 3 g/dm^3 and sodium chloride — 10 g/dm^3 with the addition of food gelatin — 5 g/dm^3. The immersion time was 5 minutes and the solution temperature was 23±1°C. The porosity was determined according to the number of the blue-colored pores per unit surface of the test sample and their size was measured. For this purpose, the sample with colored pores was placed in a Zeiss Axio Vert microscope. The size was estimated using the photographic images obtained through the microscope lens. The number and size of the pores were determined using the ZEN software product. Fig. 4 gives the enlarged image of the aluminum coating and available pores.

The digital analysis was performed for the three (3) photographic images of the surface of aluminum-coated samples with colored pores for the field size of 700×700 μm^2. The analysis data obtained for the number of pores per surface unit, average size pores and relative surface porosity were processed using the method of least squares.

The surface porosity of the aluminum coating from the substrate side and the availability of through pores in the coating were studied as follows. First, the sample section was treated with the pore-coloring solution and then it was degreased. A flat side surface of cylindrical rods was glued to the coating. Cyanoacrylate glue AKFIX-705 was used for this purpose. After gluing the rod to the aluminum coating the coating was cut through to the steel substrate along

Table 2. Description of the PAP-1 powder [36]

Grade	Granulometric composition								
	Sieve residue %, not more than (the mesh number according to GOST 6613)			Admixtures, not more than					
	+008	+0056	+0045	Fe	Si	Cu	Mg	Moisture	Fat
PAP-1	1.0	–	–	0.5	0.4	0.05	0.01	0.2	3.8

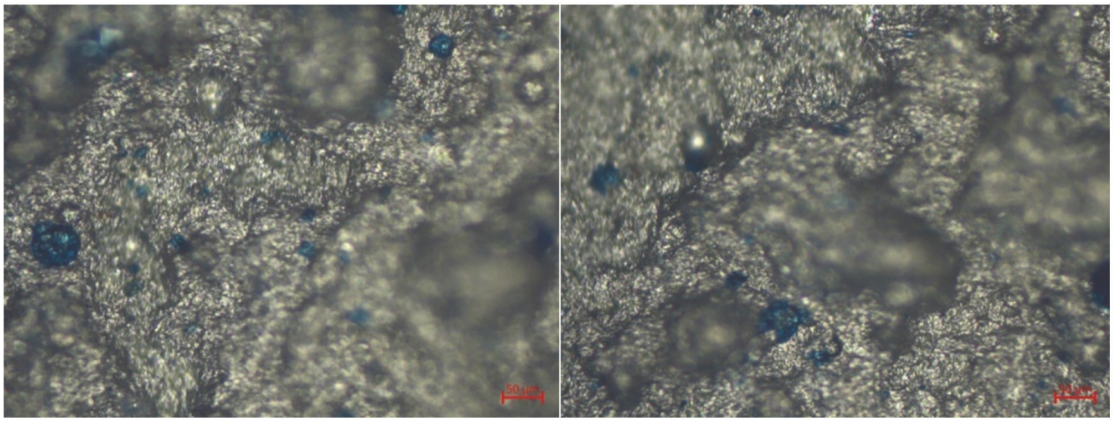

Fig. 4. Pore coloring result on the aluminum coating surface.

the contour around the rod using the engraver with a diamond drill. Afterwards the rod was torn off with the aluminum coating from the substrate. Then, to separate the aluminum coating from the rod, the rod with the aluminum coating was immersed into the medical dimexide sulfoxide to dissolve cyanoacrylate glue. After the dissolution of the glue, the sample was rinsed with kerosene and dried. Then the surface was examined under a microscope as described above.

Coating adhesion investigation method

The adhesion was studied using the method of tearing off. For this purpose, the cylindrical rods with a diameter of 6.8 and 10 mm were stuck to the coating and then the coating was cut to the substrate along the contour around the rod, as described above. The absolute error in measuring the diameter was ±0.1 mm. Due to the cutting, the effect on the tearing off the part of coating in the adjacent area was neglected. Then, the rod was torn off the sample using a special device with a gradually increasing pull-off force. The pull-off force value was recorded at the moment of tearing off. The force of separation was determined by the arrow, which made a dash on the plastic. A maximum pull-off force was defined by the end position of the dash on the plastic material. The measured values of the pull-off force and the separation surface area were used for the determination of the coating

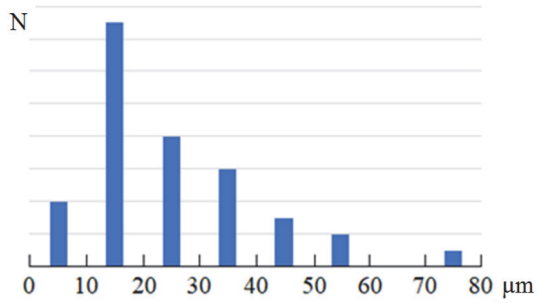

Fig. 5. Size and number distributions of the pores in the aluminum coating.

adhesion. The obtained research data were processed using the method of least squares. As the adhesion meter we used the developed device that included a lever mechanism and a dynamometer. The measurement was performed 10 times. An absolute force measurement error was ±4.9 H.

Method for studying surface roughness

The surface roughness was studied using the contactless method by measuring a change in the focal distance to the test specimen surface along the measurement line. We used a metallographic microscope PMT-3. The test specimen was fixed on the movable microscope stage. Then, the surface of the sample under study was focused in the center of the observation area. This focusing was taken as zero distance. The microscope stage screw allowed its movement

Table 3. Aluminum coating porosity

Sample No	Average diameter of pores, μm	Number of 700×700 μm^2 pores per sample, pc.	Porosity, pores/cm^2	Relative porosity, %
1	26.2	19	$2653\pm1469_{0.8}$	$2\pm1.5_{0.8}$
2	31.4	14		
3	17.5	6		

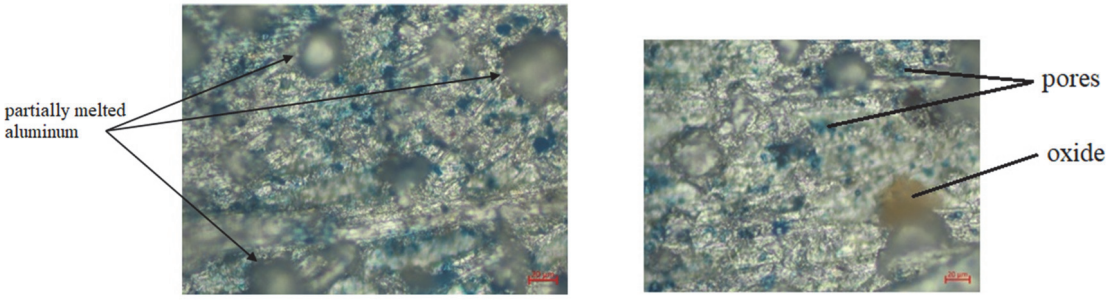

Fig. 6. View of partially melted aluminum particles (left) and the sprayed coating surface from the substrate side (pores, oxide) (right).

in one direction with a step of 200 μm. By turning the screw, focusing was carried out by distance. On completion of the focusing, the difference in the limb values of the focusing screw was compared with the zero value. Then, an appropriate limb value was expressed in terms of the depth distance. Further, this operation algorithm continued and the obtained data were used to draw the profilogram for the roughness of the coated surface.

3. Results and discussion

Table 3 shows data on the measured porosity of the surface of the aluminum coating.

The data show that the relative porosity of the coating is small. We also observe a significant scatter in the values of the pore diameter and the number of pores. This indicates an insufficient stability of the spraying process and requires the refinement of the process. Fig. 5 gives a relative distribution of the relationship between the pore number and their diameter. The data obtained show that the number of pores with a diameter of 10 to 20 μm predominates.

The external surface of the aluminum coating has been analyzed (Fig. 6). The data obtained show that the coating, which was in the melted state in the spray process, includes the spots of aluminum powder that got there in a partially melted state. Partial melting of the particles is represented by the formation of the semispherical surface. Possibly, the spray of the partially melted particles results in the formation of pores in the coating. The partial melting of powder particles can be associated with the presence of a scavenging cycle in the developed detonation gun. As a result, the remaining powder can be entrapped by the air flow during the scavenging and brought to the spray surface.

It should be noted that in addition to aluminum, the spray material also includes water and fats which create favorable conditions for the formation of the pores during evaporation. Fig. 6 (right) shows the image of the coating surface from the substrate side, where there are blue and ginger colors. The blue color corresponds to the through pores and the ginger color corresponds to areas with oxidized steel before the spraying process. This indicates insufficient surface treatment before the spray process.

The measurement data show a relatively small difference in the pull-off force for rods of the same diameter. This indicates a uniform distribution of the adhesion force of the coating and the reproducibility of the deposition quality for different samples. The measured adhesion of the coating was 1.78±0.1580.9 MPa. At the same time, with a rod diameter of 10 mm, the pull-off force was 137.2–176.4 N, with a diameter of 8 mm, the pull-off force was 78.4–98.0 N, and with a diameter of 6 mm, the pull-off force was 29.4–49.0 N.

Table 4. Comparison of the spray system parameters with the data given in [11]

Technology type	Productivity, kg/hr	Cost of the coating, GBP per 1 m^2	Coating characteristics		
			Porosity, %	Surface roughness, μm	Coating adhesion, MPa
Flame spraying	0.8	32.43	4.7	10.5	7
arc spraying	2.5	13.52	6.3	15.4	20
Plasma spraying	4.6	16.15	5.4	12.6	19
HVOF spraying	1.4	24.21	2.4	5.5	11
Air-fuel detonation spraying	>10	–	$2\pm1.5_{0.8}$	100	$1.78\pm0.158_{0.9}$

The measured roughness profilogram of the coated surface is given in Fig. 7. The obtained data showed a relatively high surface roughness that is approximately 100 μm. This indicates a non-uniform distribution of the powder during the spraying process.

The comparison of the technical and economic characteristics obtained for the spray process of aluminum coatings is given in [11]. Using these data we compare the developed technology according to the list of obtained parameters. Table 4 gives the results of such comparison. The data obtained show that the air-fuel technology of the gas-detonation spraying has certain advantages in the productivity and it also provides a low porosity. At the same time, the spray process mode requires additional studies to increase the adhesion and decrease the roughness. In addition, instead of gunpowder PAP-1, it is planned to use special gunpowder for detonation spraying. Let us estimate approximately the cost of spraying. It should be noted that the cost of the used PAP-1 powder is lower than that of special spray powders. Namely, the cost of the powder is within 20 pounds per 1 kg. The plant uses propane at a rate of 4 kg/hour for its operation, which in terms of GBP means 4 pounds per hour. The consumed electric power is 20 kW and in terms of GBP it corresponds to 2 pounds per hour. Taking into consideration the cost of the plant, i.e. 20 000 GBP and the operation resource of 5000 hours we get a depreciation cost of 4 pounds per hour. Taking into consideration the payment for work in the amount of 30 pounds per hour we get a total spray cost in the amount of 21.3 pounds per kilogram. For the coating layer of 200 μm thick we need 0.54 kg/m^2 of aluminum powder. Hence, we get a coating spray cost equal to 9.4 GBP per 1 m^2. Therefore, the estimated coating cost for the developed technology is the lowest and it is reasonable to continue the development and improvement of this technology.

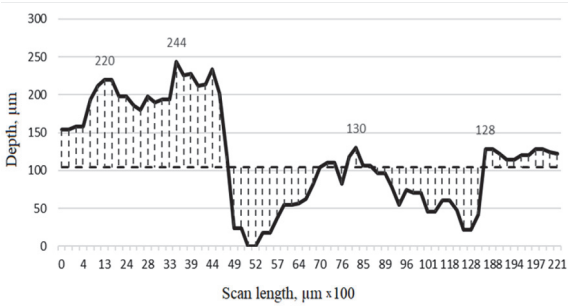

Fig. 7. Sprayed surface roughness profilogram.

4. Conclusion

The characteristics of the air-fuel technology used for the gas-detonation spraying were compared to those for other types of the technology using the data of the aluminum spray onto steel. The comparison data showed that at this stage of studies, the air-fuel technology used for the gas-detonation spraying has certain advantages in the productivity and provides a low porosity. At the same time, it requires additional improvement of the spray mode to increase the adhesion and decrease the roughness. The estimated cost of the coating applied using this technology is the lowest. Therefore it is reasonable to continue the development and improvement of this particular spray process.

References

1. A.Hasui, O.Morigaki, Naplavka i Napylenie, Mashinostroenie, Moscow (1979) [in Russian].
2. V.Shatt, Poroshkovaja Metallurgija. Spechennye i Kompozicionnye Materialy, Metallurgija, Moscow (1983) [in Russian].
3. V.N.Antsiferov, G.V.Bobrov, L.K.Druzhinin et al., Poroshkovaya Metallurgiya i Napylennye Pokrytiya, Metallurgija, Moscow (1987) [in Russian].

4. A.J.Panas, C.Senderowski, B.Fikus, *Thermochim Acta*, 676 (2019). https://doi.org/10.1016/j.tca.2019.04.009.
5. C.Senderowski, A.J.Panas, B.Fikus et al., *Materials*, **14**, 23 (2021). https://doi.org/10.3390/ma14237443.
6. V.S.Panov, A.M.Chuvilin, V.A.Fal'kovskij, Tehnologija i Svojstva Spechennyh Tverdyh Splavov i Izdelij iz Nih, MISIS, Moscow (2004) [in Russian].
7. S.S.Bartenev, Ju.P.Fed'ko, A.I.Grigor'ev, Detonacionnye Pokrytija v Mashinostroenii, Mashinostroenie, Leningrad (1982) [in Russian].
8. P.A.Vitjaz', B.C.Ivashko, Z.D.Manojlo et al., Teorija i Praktika Gazoplamennogo Napylenija, Navuka i tjehnisa, Minsk (1993) [in Belarus].
9. Ju.A.Harlamov, M.H.Shorshorov, V.V.Kudinov et al., Primenenie Detonatsii v Gazakh dlya Naneseniya Pokrytiy, Fizika Goreniya i Vzryva, SO AN SSSR, Moscow (195 ? ????) [in Russian].
10. V.V.Kudinov, G.V.Bobrov, Nanesenie Pokrytij Napyleniem. Teorija, Tehnologija i Oborudovanie, Metallurgija, Moscow (1983) [in Russian].
11. A.Y.Kulik, Y.S.Borisov, A.S.Mnukhin et al., Gazotermicheskoe Napylenie Kompozitsionnykh Poroshkov. Gas-Thermal Deposition of Composite Powders, Mashinostroenie, Leningrad (1985) [in Russian].
12. Ju.S.Borisov, Ju.A.Harlamov, S.L.Sidorenko et al., Gazotermicheskie Pokrytija iz Poroshkovyh Materialov, Naukova Dumka, Kyiv [Ukraine].
13. S.Shrestha, A.Sturgeon, EUROCORR, 2005 (2005).
14. https://www.metallisation.com/product-category/flame-spray/.
15. https://www.metallisation.com/product-category/arc-spray/.
16. R.Grinon-Echaniz, P.Refait, M.Jeannin et al., *Corros SCI*, 187 (2021). https://doi.org/10.1016/j.corsci.2021.109514.
17. R.G.Echaniz, S.Paul, R.Thornton, *Mater.Corros.*, **70**, 6 (2019). https://doi.org/10.1002/maco.201810764.
18. https://www.metallisation.com/products/arc spray-528e-icc-high-throughput/.
19. A.Castro-Vargas, S.Gill, S.Paul, *Surfaces*, 5 (2022). https://doi.org/10.3390/surfaces5010005.
20. B.Syrek-Gerstenkorn, S.Paul, A.J.Davenport, *Coatings*, **10**, 267 (2020). https://doi.org/10.3390/coatings10030267.
21. M.H.AbdMalek, N.H.Saad, S.K.Abas et al., *IOP Conf.Ser-Mat.Sci*, **46**, 1 (2013). doi:10.1088/1757-899X/46/1/012028.
22. K.V.Korytchenko, O.Y.Hichlo, I.O.Belousov et al., *AIP Conf.Proc.*, **27**, 1 (2020). https://doi.org/10.15407/fm27.01.224.
23. Korytchenko, R.Tomashevskiy, I.Varshamova et al., KhPIWeek, (2020). doi: 10.1109/KhPIWeek51551.2020.9250172.
24. K.Korytchenko, D.Samoilenko, D. Dubinin et al., *Mater.Sci.Forum*, 1038 (2021). https://doi.org/10.4028/www.scientific.net/msf.1038.500.
25. K.Korytchenko, P.Krivosheyev, D.Dubinin et al., *EEJET*, **4**, 5/100 (2021). doi:10.15587/1729-4061.2019.175333
26. K.Korytchenko, R.S.Tomashevskyi, I.Varshamova et al., *Probl.Atom.Sci.Tech.*, **4**, 122 (2019). doi:10.46813/2019-122-116
27. K.V.Korytchenko, A.M.Kasimov, V.I.Golota et al., *Probl.Atom.Sci.Tech.*, **6**, 118 (2018).
28. K.V.Korytchenko, I.S.Varshamova, D.V.Meshkov et al., *Probl.Atom.Sci.Tech.*, **1**, 131 (2021). doi:10.46813/2021-131-092.
29. D.Dubinin, K.Korytchenko A.Lisnyak et al., *EEJET*, **2**, 10/92 (2018). https://doi.org/10.15587/1729-4061.2018.127865.
30. P.Srihari, G.Sai Prasad, B.V.N.Charyulu et al., *Intern.Journal of Recent Advances in Mechanical Engineering*, 3 (2014). doi:10.14810/ijmech.2014.3303.
31. D.Rybin, V.Yu.Ul'yanitskii, I.S.Batraev, *Combust.Explo Shock*, **56**, 3 (2020). doi:10.1134/S0010508220030120.
32. M.Mitu, V.Brinzea, A.Musuc et al., *U.P.B.Sci.Bull., Series B*, **73**, 3 (2011).
33. V.I.Tarzhanov, I.V.Telichko, V.G.Vil'danov et al., *Combust Explo Shock*, 42 (2006). https://doi.org/10.1007/s10573-006-0060-4.
34. F.A.Baum, K.P.Stanjukovich, B.I.Shehter, Fizika Vzryva, Izd-vo Fiziko-matematicheskoj Literatury, Moscow (1959) [in Russian].
35. N.Bheekhun, A.B.D.R.binAbuTalib, H.Hasini et al., *Appl.Mech.Mater.*, 564 (2014). https://doi.org/10.4028/www.scientific.net/AMM.564.240.
36. GOST 5494-95 Pudra Aljuminijeva. Tehnichni Umovy.
37. DSTU 2491-94 Pokryttja Metalevi ta Nemetalevi Neorganichni. Terminy ta Vyznachennja.